



Landing Trajectory Design for UAV Considering Control Restrictions and Landing Speed

Ngo Van Toan (Corresponding Author)

Faculty of Aeronautical engineering, Air defence-air force Academy, Son Tay, Ha Noi, Viet Nam

Email: toantbkh@gmail.com

Doan The Tuan

Faculty of Control engineering, Le Quy Don Technical University, 236 Hoang Quoc Viet, Ha Noi city, Viet Nam

Pham Ngoc Van

Faculty of Control engineering, Le Quy Don Technical University, 236 Hoang Quoc Viet, Ha Noi city, Viet Nam

Nguyen Thanh Tung

Faculty of Control engineering, Le Quy Don Technical University, 236 Hoang Quoc Viet, Ha Noi city, Viet Nam

Nguyen Ngoc Dien

Faculty of Control engineering, Le Quy Don Technical University, 236 Hoang Quoc Viet, Ha Noi city, Viet Nam

Article History

Received: 29 June, 2021

Revised: 15 July, 2021

Accepted: 27 July, 2021

Published: 29 July, 2021

Copyright © 2021 ARPG
& Author

This work is licensed
under the Creative
Commons Attribution
International



BY: [Creative Commons
Attribution License 4.0](https://creativecommons.org/licenses/by/4.0/)

Abstract

The article presents a method for designing the trajectory of the UAV in space, taking into account the restriction on control. The chosen optimal controls are namely normal overload with restrictions, tangential overload with restrictions and lateral overload. The Pontryagin maximum principle allows the transition of the optimal control problem to a boundary value problem. The parameter continuation method is applied to solve the boundary problem. The article results reveal reference trajectories in different cases of UAV landing. This result allows the design of reference trajectories for the UAV to attain the highest landing efficiency.

Keywords: Control restriction; Reference trajectory; Parameter continuation method; Normal overload; Tangential overload; Lateral overload.

1. Introduction

During the process of landing, the value of UAV landing speed is critically significant in case of landing on short runway or emergency landing... UAV is expected to land with a small landing speed; otherwise, the large landing speed may lead to unsafety circumstances such as the UAV going off the runway, the UAV may flip or change direction when landing. In addition to landing speed, control restrictions also have a significant effect on landing quality. During the landing process, the situation is diverse, and the drones should closely abide by some reference trajectories to achieve efficient landing with respect to some performance indices [1, 2]. Therefore, in this article, the authors establish a reference trajectory for UAV with consideration of values of different landing speed and optimal controls namely normal overload with restrictions, tangential overload with restrictions and lateral overload. This problem can be handled by 2 methods: analytical and numerical one. The analytical method offers feedback control, however, depending on the boundary conditions coupling with the restricted control during flight, seeking for an optimal control would be of arduousness. With the aim to establish a reference trajectory in the service of landing cases, the authors select the numerical method to solve the bespoke problem. This method burgeons results in a quick manner in case of restricted control and variable boundaries. For better application of the numerical method, the authors convert the optimal control problem to the boundary problem, the parameter continuation method [3-7] is used to successfully handle the boundary problem. The simulation results show that the UAV lands with different speed values and the control is within the allowable range.

2. Algorithm Establishment

2.1. Optimal Landing Trajectory

The system of equations of UAV movement in space includes the following differential equations [3]:

$$\begin{cases} \dot{V} = g \cdot (n_x - \sin \theta) \\ \dot{\theta} = \frac{g}{V} \cdot (n_y - \cos \theta) \\ \dot{\varphi} = -\frac{g}{V} \cdot \frac{n_z}{\cos \theta} \\ \dot{x} = V \cdot \cos \theta \\ \dot{y} = V \cdot \sin \theta \\ \dot{z} = -V \cdot \cos \theta \cdot \sin \varphi \end{cases} \quad (1)$$

in which:

V – velocity of UAV

θ - flight path angle

φ - heading angle

x, y, z - UAV coordinates

g - gravity acceleration ($g = 9,80665 \text{ m/s}^2$)

n_x, n_y, n_z - respectively corresponding tangential overload, normal overload, lateral overload.

$X = [V, \theta, \varphi, x, y, z]^T$ - UAV state vector

Consider control $u = [n_x, n_y, n_z]^T$, then the cost function given in Bolza form is:

$$J = 0,5 \int_{t_0}^{t_f} u^T \cdot k^{-2} \cdot u dt.$$

In which:

$k^2 = \text{diag}(k_1^2, k_2^2, k_3^2)$ - parameters of the cost function

t_0 и t_f - the beginning and the end of the flight

$V(t_f), \theta(t_f), \varphi(t_f), x(t_f), y(t_f), z(t_f)$ - boundary condition at the end time

Then, the Halminton function holds the form [6] as follow:

$$H = P_V \cdot g \cdot (n_x - \sin \theta) + P_\theta \cdot \frac{g}{V} \cdot (n_y - \cos \theta) - P_\varphi \cdot \frac{g}{V} \cdot \frac{n_z}{\cos \theta} + P_x \cdot V \cdot \cos \theta + P_y \cdot V \cdot \sin \theta - P_z \cdot V \cdot \cos \theta \cdot \sin \varphi - \frac{1}{2} \cdot k_1^{-2} \cdot n_x^2 - \frac{1}{2} \cdot k_2^{-2} \cdot n_y^2 - \frac{1}{2} \cdot k_3^{-2} \cdot n_z^2.$$

and the equations for co-state variables have the form:

$$\begin{cases} \dot{P}_V = -\frac{\partial H}{\partial V} = P_\theta \cdot \frac{g}{V^2} \cdot (n_y - \cos \theta) - P_\varphi \cdot \frac{g}{V^2} \cdot \frac{n_z}{\cos \theta} - P_x \cdot \cos \theta \cdot \cos \varphi - P_y \cdot \sin \theta + P_z \cdot \cos \theta \cdot \sin \varphi \\ \dot{P}_\theta = -\frac{\partial H}{\partial \theta} = P_V \cdot g \cdot \cos \theta - P_\theta \cdot \frac{g}{V} \cdot \sin \theta + P_\varphi \cdot \frac{g}{V} \cdot \frac{n_z}{\cos^2 \theta} \cdot \sin \theta + P_x \cdot V \cdot \sin \theta \cdot \cos \varphi - P_y \cdot V \cdot \cos \theta - P_z \cdot V \cdot \sin \theta \cdot \sin \varphi \\ \dot{P}_\varphi = -\frac{\partial H}{\partial \varphi} = P_x \cdot V \cdot \cos \theta \cdot \sin \varphi + P_z \cdot V \cdot \cos \theta \cdot \cos \varphi \\ \dot{P}_x = -\frac{\partial H}{\partial x} = 0 \\ \dot{P}_y = -\frac{\partial H}{\partial y} = 0 \\ \dot{P}_z = -\frac{\partial H}{\partial z} = 0 \end{cases} \quad (2)$$

The authors find the optimal control at each time that makes Hamilton function H reach the maximum

$$\max_{u \in U} H(x^*, u, P^*, t) = H(x^*, u^*, P^*, t).$$

Due to the fact that n_z is within the allowable range when conducting the survey or at the beginning of the landing phase, the movement direction of the UAV is asymptotical to or coincided with the runway direction, so n_z in the given article is unrestricted. From the optimal condition $\frac{\partial H}{\partial n_z} = 0$, the authors gain the control:

$$n_z = -P_\varphi \cdot \frac{g}{V \cdot \cos \theta} \cdot k_3^2. \text{ With } n_x, n_y, \text{ the writers found in maximum principle in case of restricted control:}$$

$\max_{n_x \in N_x, n_y \in N_y} H(x^*, n_x, n_y, n_z^*, P^*, t) = H(x^*, n_x^*, n_y^*, n_z^*, P^*, t)$. Accordingly, the system of equations for the UAV full movement includes the combination of the system of equations (1) and (2).

Then, there goes an essence to find the initial condition $P_V(t_0), P_\theta(t_0), P_\varphi(t_0), P_x(t_0), P_y(t_0), P_z(t_0), t_f$ which matches the boundary condition $V(t_f) = V_f, \theta(t_f) = \theta_f, \varphi(t_f) = \varphi_f, x(t_f) = x_f, y(t_f) = y_f, z(t_f) = z_f, H(X, P, t_f) = 0$.

With $V_f, \theta_f, \varphi_f, x_f, y_f, z_f$ - desired value given at the end time t_f .

To solve the boundary problem, the authors use the method of parameter continuation.

2.2. Parameter Continuation Method

The essence of the parameter continuation method lies at the formal reduction of the considered boundary value problem to the Cauchy problem [4-7]. The boundary problem for a dynamic system with boundary conditions can be represented as an equation for the residuals at the right end of the trajectory:

$$\mathbf{f}(\mathbf{z}) = 0 \tag{3}$$

In which:

$\mathbf{z} = [P_V(t_0) \ P_\theta(t_0) \ P_\varphi(t_0) \ P_x(t_0) \ P_y(t_0) \ P_z(t_0) \ t_f]^T$ - vector of unknown parameters of the boundary value problem;

$$\text{The residual vector: } f(\mathbf{z}) = \begin{bmatrix} V(t_f) - V_f \\ \theta(t_f) - \theta_f \\ \varphi(t_f) - \varphi_f \\ x(t_f) - x_f \\ y(t_f) - y_f \\ z(t_f) - z_f \\ H(t_f) \end{bmatrix} = 0$$

At some initial approximation for the unknown parameters of the boundary value problem \mathbf{z}_0 , the residual vector is calculated as (3):

$$\mathbf{f}(\mathbf{z}_0) = \mathbf{b} \tag{4}$$

Considering the immersion of equation (4) in a one-parameter family:

$$\mathbf{f}(\mathbf{z}) = (1 - \tau)\mathbf{b} \tag{5}$$

in which: τ is the continuation parameter, and the writers represent the vector \mathbf{z} as a function of this parameter: $\mathbf{z} = \mathbf{z}(\tau)$, moreover $\mathbf{z}(0) = \mathbf{z}_0$ from equation (4). They require equality (5) for any $0 \leq \tau \leq 1$. Obviously, for $\tau = 0$, equation (5) coincides with (4), and for $\tau = 1$ - the equation for residuals for the desired boundary value problem (3).

Differentiating equation (5) with respect to the continuation parameter τ and solving the resulting expression for the derivative $d\mathbf{z}/d\tau$, we obtain a formal reduction of equation (3) to the Cauchy problem:

$$\mathbf{f}(\mathbf{z}) = (1 - \tau)\mathbf{b} \Rightarrow \frac{d\mathbf{z}}{d\tau} = - \left(\frac{\partial \mathbf{f}}{\partial \mathbf{z}} \right)^{-1} \mathbf{b}, \tag{6}$$

$$\mathbf{z}(0) = \mathbf{z}_0, \quad 0 \leq \tau \leq 1.$$

Obviously, integrating (6) over τ from 0 to 1, it is of ease to define the desired vector of unknown parameters of the boundary value problem (3) in the form $\mathbf{z} = \mathbf{z}(1)$.

$$\int_0^1 \frac{d\mathbf{z}}{d\tau} d\tau = - \int_0^1 \left(\frac{\partial \mathbf{f}}{\partial \mathbf{z}} \right)^{-1} \mathbf{b} d\tau \Leftrightarrow \mathbf{z}(1) = \mathbf{z}(0) - \int_0^1 \left(\frac{\partial \mathbf{f}}{\partial \mathbf{z}} \right)^{-1} \mathbf{b} d\tau$$

Thus, the value of the original parameter vector $\mathbf{z}(1)$ has been found.

3. Simulation Results

Calculating aerodynamically with specific UAV model: UAV mass $m = 56.5$ Kg, wing area $S = 1.05$ m, the results are limited to $n_x \in [-0,82 \ 1]$, $n_y \in [-0,4 \ 1,2]$. The value of the parameters of the cost function is chosen as follows: $k_1 = 0,1$; $k_2 = 0,1$; $k_3 = 0,1$.

Case 1: Survey with a fixed initial state and variable landing speed

The initial state of UAV with: $V(0) = 50$ m/s; $\theta(0) = 0$ radian; $\varphi(0) = 0$ radian; $x(0) = 0$ m; $y(0) = 1000$ m; $z(0) = 800$ m.

The desired state of UAV: $V_f = 25;35;45$ m/s; $\theta_f = 0$ radian; $\varphi_f = 0$ radian; $x_f = 2000$ m; $y_f = 0$ m; $z_f = 0$ m.

With the use of Matlab 2015 application, the results are received as follows:

Figure-1. UAV trajectory with variable V_f

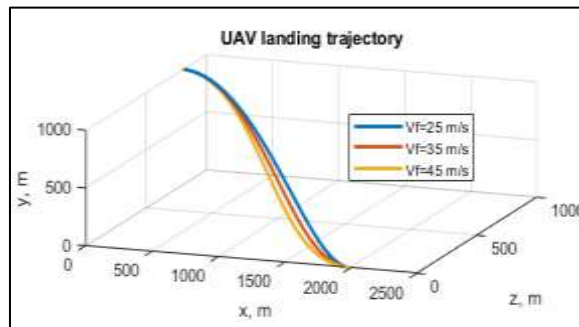


Figure-2. Hamilton function with variable V_f

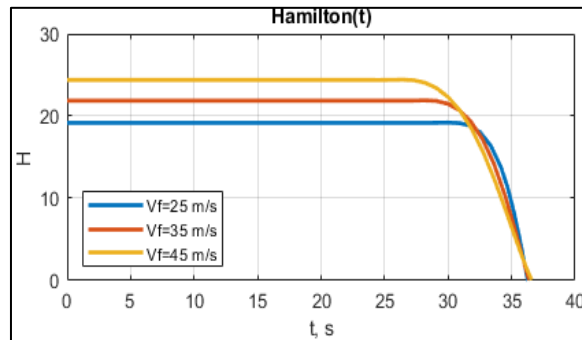


Figure 1 illustrates the UAV trajectory in space corresponding to various landing speeds. It can be apparently seen that the higher the landing speed is the more tension the trajectory has.

The results shown indicate that the value of the Hamilton function at the end t_f is close to 0 in all cases, which demonstrates that the landing time has been optimized (Figure 2). The values of in 3 different cases landing speed respectively take the values 36,27; 36,36; 36,56. Hence, the landing time with different landing speeds is almost unchanged.

Figure 3 and figure 4 depict the change of UAV trajectorial tilt and flight path angle in real time corresponding to different landing speeds V_f . The figure visualizes the angle change in almost the same cases.

Figure-3. UAV tilt angle with different V_f

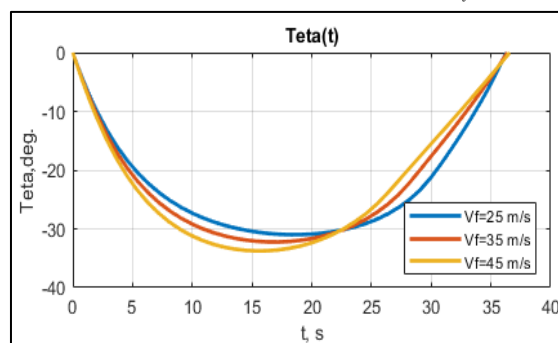


Figure-4. UAV flight path angle with different V_f

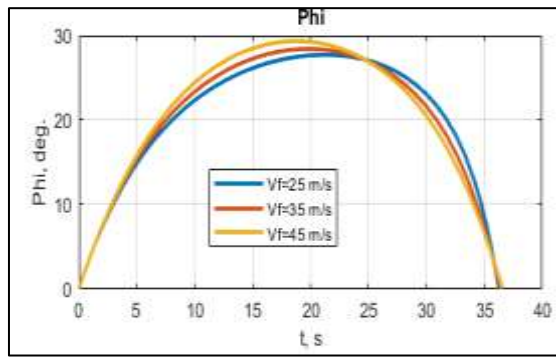


Figure 5 delineates the speed change of UAV in time corresponding to different V_f . It unveils that the lower the landing speed is in 0-25s stage, the higher the UAV landing speed becomes.

Figure-5. UAV velocity with different V_f

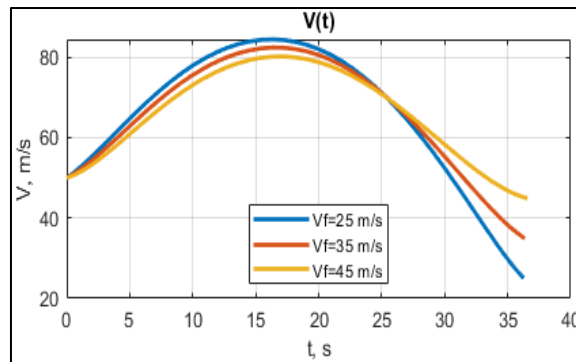


Figure-6. Change of n_x with different V_f

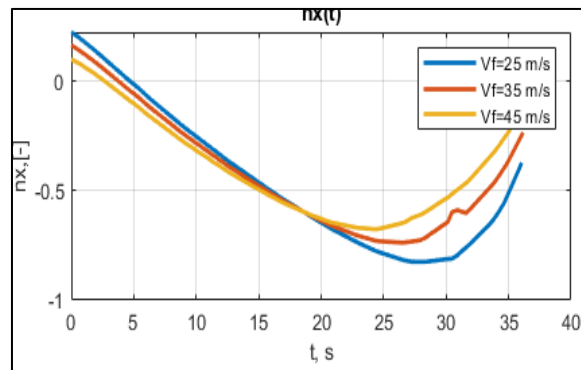
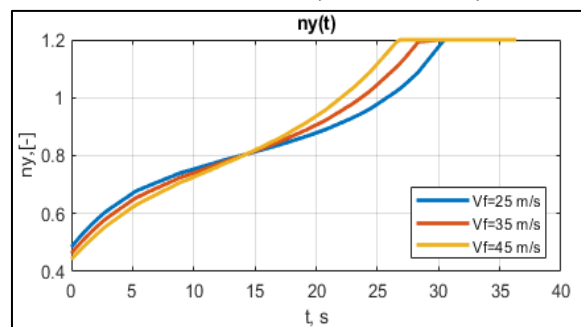


Figure 6, 7 and 8 presents the change of control n_x, n_y, n_z in time with different landing speed V_f . It can be clearly seen from Figure 6 that from 20s onwards, the lower the landing speed is, the higher the absolute value n_x is. In case $V_f = 25$ m/s, in the range from 27 to 30s, the value n_x reaches the extreme since the problem in consideration restricts the control for n_y .

Figure-7. Change of n_y with different V_f



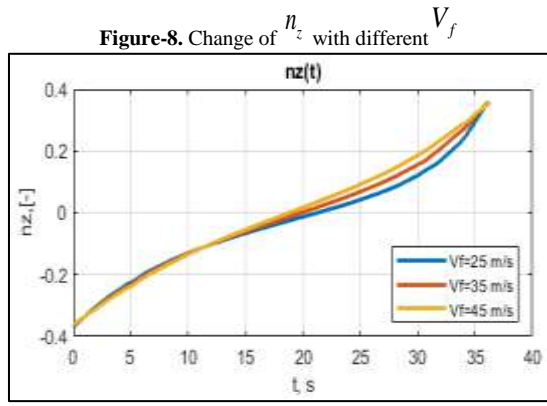


Figure 7 shows that at the end in 3 cases, value of n_y reaches the extreme and the lower V_f is, the longer it takes n_y to reach the extreme. Whereas, figure 8 indicates values of n_z are approximately equal at the beginning (end) time at different landing speeds.

Case 2: Changing initial state of UAV and fixed landing speed

When changing the initial location of UAV with:

$$(y_0 = 600\text{ m}, z_0 = 600\text{ m}; y_0 = 800\text{ m}, z_0 = 800\text{ m}; y_0 = 1000\text{ m}, z_0 = 1000\text{ m})$$

the results gained after running the program with the landing speed $V_f = 35\text{ m/s}$ are as follows:

Figure 9 exhibits the UAV trajectory in space when the initial location was changed. It can be clearly seen that value of Hamilton function at the end t_f approaches 0 (Figure 10).

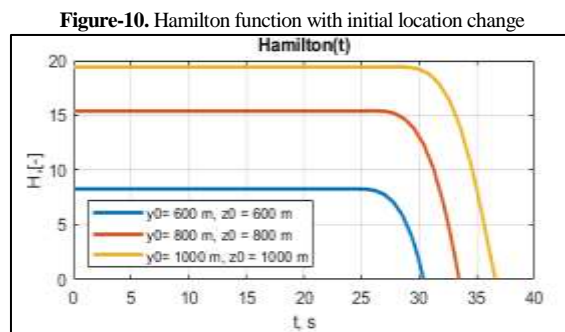
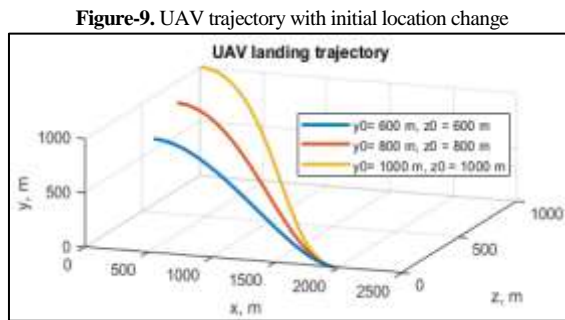


Figure 11 and 12 illustrate the change of UAV tilt and flight path angle when its initial location was changed. It indicates that the larger the distance between the UAV at the initial time and the landing position, the greater the change in its UAV tilt and flight path angle.

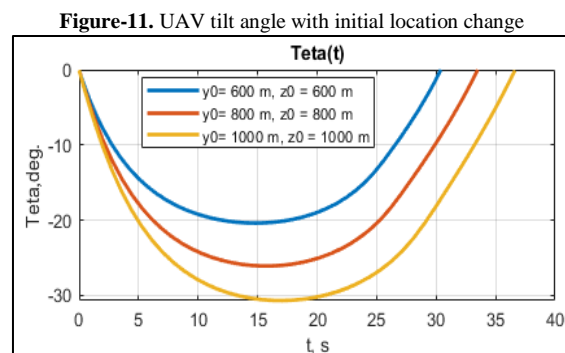


Figure-12. UAV flight path angle with initial location change

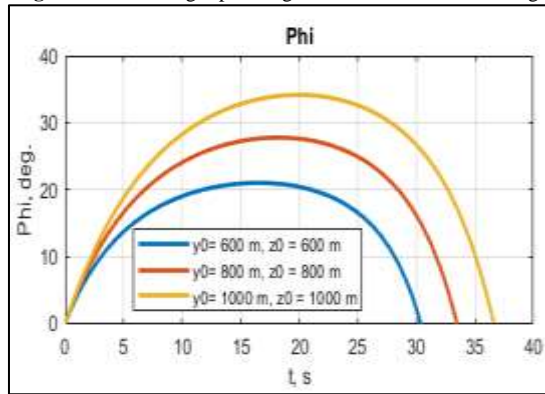


Figure 13 depicts the change of UAV velocity in time when its initial location was changed.

Figure-13. UAV speed with initial location change

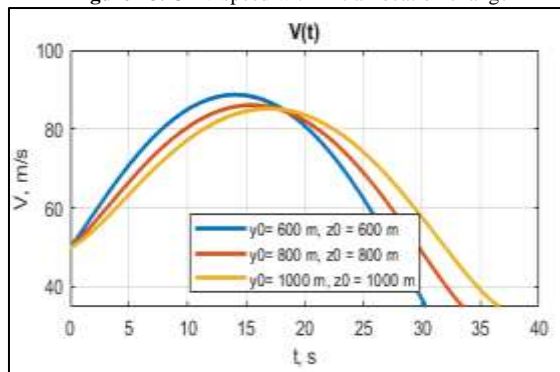


Figure-14. Change of n_x in time with initial location change

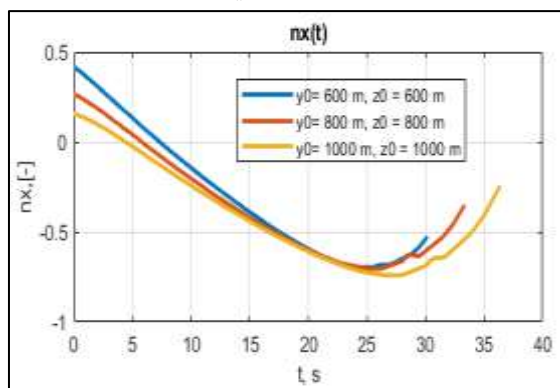


Figure 14, 15 and 16 present the change of control n_x, n_y, n_z in time when the initial location was changed. It demonstrates that the value range of n_x and total flight time t_f also increases when the initial distance from UAV to landing position extends.

Figure-15. Change of n_y in time with initial location change

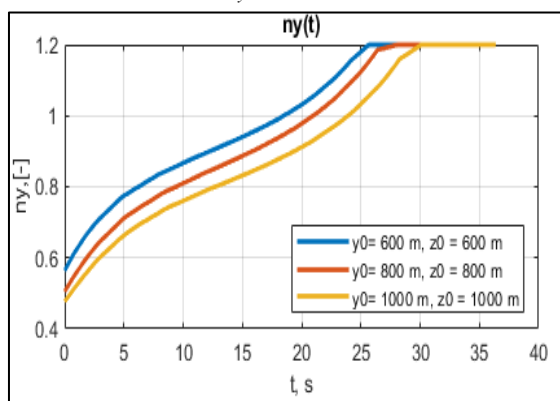
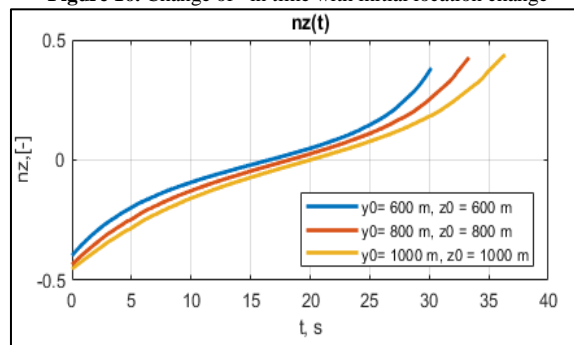


Figure 16. Change of $nz(t)$ in time with initial location change

4. Conclusion

Via surveying the flight trajectory, the authors may state that in case 1, landing with low speed holds more advantages in emergency circumstances in which the aircraft encounters alarming problems and must land on a short runway, but the decreasing landing speed comes with the increase of tangential overload. Hence, the actualization of flight will be of difficulty if the UAV fails to meet the tangential overload as calculated during flight. In case 2, with different beginning positions, the landing trajectory would be variable, the more the landing direction deviates from the runway direction, the greater the control energy consumes. The research results claims that different flight trajectories can be designed and the feasibility may be evaluated when realizing flight trajectory, thereby offering reference trajectories. In this article, there remains a point mis-considering the noise influence during flight since using numerical method instead of analytical method would reveal several disadvantages with noise involvement. Therefore, the authors are expected to consider the impact of noise in flight in the coming studies.

References

- [1] Horla, D. and Cieślak, J., 2020. "On obtaining energy-optimal trajectories for landing of uavs." *Energies*, vol. 13, p. 2062.
- [2] Visintini, A., Perera, T. D. P., and Jayakody, D. N. K., 2021. "3-d trajectory optimization for fixed-wing uav-enabled wireless network." *IEEE*, vol. 9, pp. 35045-35056.
- [3] Aleksandrov A. A., 2009. "Optimal control of aircraft, taking into account restrictions on control". The PhD thesis, p. 134.
- [4] Dikusar, V. V., Koshka, M., and Figura, A., 2011. "A parameter extension method for solving boundary value problems in optimal control theory." *Differential Equations*, vol. 37, pp. 479–484.
- [5] Enright, W. H., 2000. "Continuous numerical methods for ODEs with defect control." *Journal of Computational and Applied Mathematics*, vol. 125, pp. 159-170.
- [6] Petukhov, V. G., 2012. "Method of continuation for optimization of interplanetary low-thrust trajectories." *Cosmic Research*, vol. 50, pp. 249-261.
- [7] Shalashilin V. I., Kuznetsov, E. B., 1999. "Parameter continuation method and the best parametrization", Moscow: Editorial URSS, p. 224.